Review of AMTD paper, Manuscript Number: amt-2010-201

Response to the comments of Reviewer #1

We thank the reviewer for the detailed review and the helpful and constructive comments which we fully took into account in the revision of the paper. Please see our detailed response below.

General comment

I would like to see an additional discussion on correlations and vertical resolution. Also, I suggest to at least discuss the range above 34 km. RO data is now used in assimilation models up to about 50 km, thus error models would be very useful higher up.

We appreciate this valuable comment and agree with the reviewer that knowledge on error characteristics of bending angle and refractivity above 35 km is important, especially for assimilation purposes. We thus include this information in the revised paper and extend the error model accordingly for bending angle and refractivity, which are the two key variables suitable for assimilation given their useful observation information also above 35 km.

We compare error characteristics of raw and optimized bending angle profiles. The latter is affected by model information at higher altitudes, which penetrates down in the Abel integral and affects refractivity error characteristics above 30 km. Since the WEGC profiles are not operationally available above 35 km, we restrict this analysis to UCAR data but note that the error correlation model is applicable to WEGC data as well.

In Figure 1 (left panel), we substituted WEGC optimized bending angle error characteristics for UCAR raw bending angle error characteristics and show this plot up to 50 km. Furthermore, we included an additional Figure, which shows error characteristics and error correlation functions and their models for raw bending angle, optimized bending angle, and refractivity up to 50 km (new Figure 7 in the revised document, Figure 1 here). The error correlations are found consistent with the results of Steiner and Kirchengast (2005) and Steiner et al. (2006) and their model formulations for error correlation functions. For the reviewer's convenience we add Figure 2, which shows error correlation functions for raw bending angle, refractivity, dry pressure, dry geopotential height, and dry temperature.

In the abstract of the manuscript we added the following sentence:

For bending angle and refractivity we also include formulations for error correlations in order to enable modeling of full error covariance matrices for these primary data assimilation variables.

In the manuscript we added the following paragraphs in Sect. 3.4:

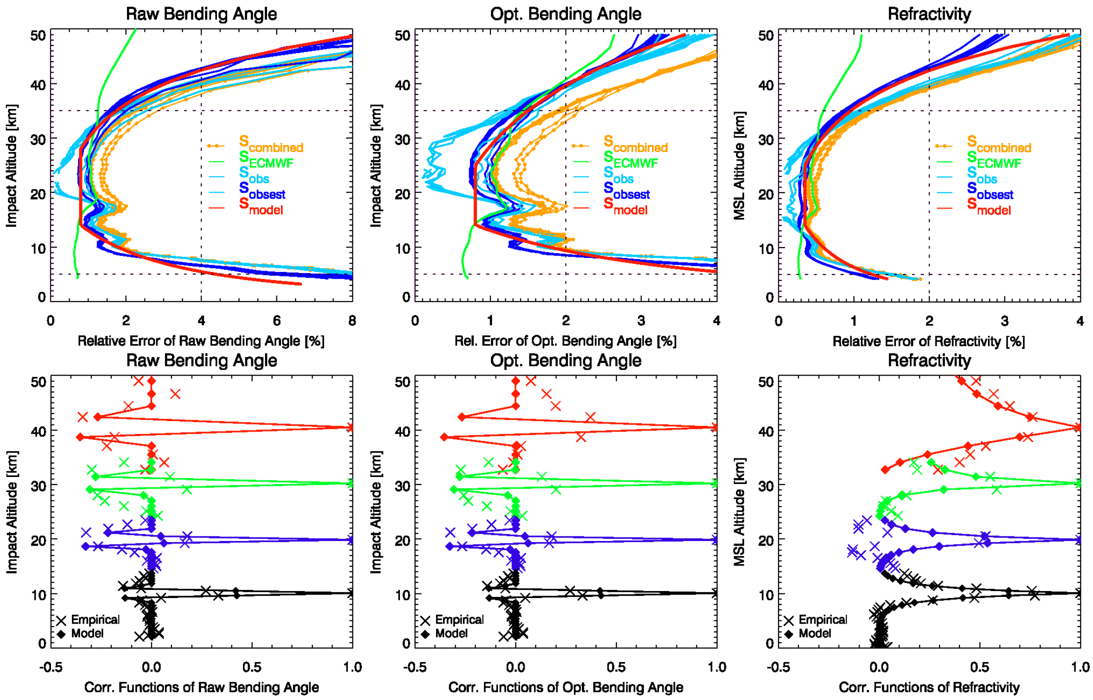

Figure 1: UCAR global error estimates (top) and error correlation functions (bottom) in July 2008 for raw and optimized bending angle as well as for refractivity up to 50 km. Empirical (x-symbols) and modeled (connected diamonds) correlation functions are shown based on GRACE-A data for four representative altitude levels from 10 km to 40 km.

The error model is applicable up to 50 km for raw bending angle, optimized bending angle, and refractivity (up to 35 km for the other parameters). In addition, information on the error correlation structure is provided for these variables, for construction of error covariance matrices and their use, e.g., in NWP assimilation systems. Figure 7 shows global error estimates, error correlation functions and their models for UCAR raw and optimized bending angles, as well as refractivity up to 50 km.

The impact of statistical optimization can clearly be seen comparing raw and optimized bending angle (Fig. 7, top panels). While the raw bending angle observational error exceeds 8 % near 45 km, the observational errors of the statistically optimized bending angle and of refractivity remain smaller than 4 % up to 50 km (larger errors can occur in the lower troposphere). To account for the impact of background information at high altitudes, the observational error model for the optimized bending angle uses a lower z_{bot} and a larger H_{S0} and ΔH_{S}.

The bottom panels of Fig. 7 show the empirical and modeled error correlation functions. Very good agreement with the results obtained by Steiner and Kirchengast (2005) is given and we follow their approach to model error correlations for raw bending angle by using a Mexican Hat function of the form

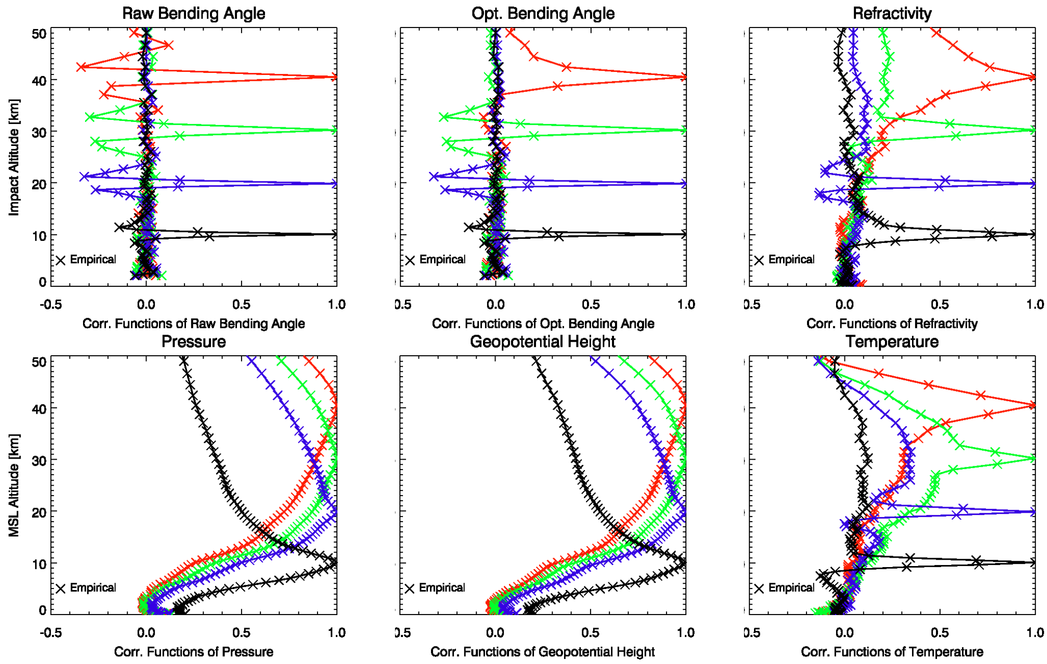

Figure 2: Error correlation functions for ≈10 km, ≈20 km, ≈30 km, and ≈40 km are shown for GRACE-A raw bending angle, optimized bending angle, refractivity, dry pressure, dry geopotential height, and dry temperature in July 2008.

$$\mathbf{S} = S_{ij} = s_i s_j \cdot \left(1 - \frac{(z_i - z_j)^2}{(c \cdot L)^2}\right) \cdot \tilde{f}, \tag{1}$$

where $\mathbf{S}$ is the error covariance matrix with elements S_{ij}, s_i and s_j are the standard deviations at height levels z_i and z_j, respectively, c is a stretching factor, and $L = L(z)$ the height dependent correlation length. The function $\tilde{f}$, representing the Gaussian exponential factor in the Mexican Hat function, is modeled for robust invertability of $\mathbf{S}$ after Gaspari and Cohn (1999) as formulated in detail by Steiner and Kirchengast (2005).

We choose c to be $c = 1.0$ below 14 km (hardly any overshooting of error correlations that allows error correlation values to be negative), linearly decreasing to $c = 0.8$ at 50 km (stronger overshooting). The correlation length L was estimated to be 1.5 km at 50 km, linearly decreasing to 0.7 km at 14 km and kept at this value downwards. The error correlation model obtained from raw bending angle data is also plotted for cross-check for the statistically optimized bending angle, which is generally not used for assimilation. The model almost perfectly fits also these data up to the 30 km level below which background information is negligible, but above the influence of background information becomes noticeable through a much larger error correlation length and no overshooting. Error correlations at these altitude levels would require a different model such as, e.g., applied for refractivity.

Refractivity error correlations are modeled after Steiner et al. (2006) using an exponential function of the form

$$\mathbf{S} = S_{ij} = s_i s_j \cdot \exp\left(-\frac{|z_i - z_j|}{L(z)}\right), \tag{2}$$

where the correlation length $L(z)$ was estimated to be 1 km up to 30 km altitude and then linearly increasing to $L = 10$ km at 50 km. This increase accounts for an increasingly larger amount of background information at higher altitudes.
The error correlation functions are also usable for the WEGC data over their domain of availability up to 35 km.

To address the vertical resolution of RO profiles, we added a paragraph at the end of Section 2.1.2. It reads:

Given the type of filtering involved, the vertical resolution of both UCAR and WEGC profiles is about 1 km from near 5 km up to an altitude of 30 km, above which the resolution can be approximated as increasing linearly to reach 2 km at 50 km altitude.

Minor comments

- *Page 3: The GRAS SAF actually provides the refractivity data in near real-time, EUMETSAT the bending angle. Please clarify this.*

  Thanks for this comment, we corrected the statement to:

  Current data assimilation centers assimilate either RO bending angle or RO refractivity as provided by ... the European Organization for the Exploitation of Meteorological Satellites (EUMETSAT) (MetOp/GRAS bending angle), and the Global Navigation Satellite System Receiver for Atmospheric Sounding–Satellite Application Facilities (GRAS-SAF) (MetOp/GRAS refractivity) in near-real time.

- *Page 4: "For noise reduction ... " This initialization applies only for refractivity calculation, the bending angles are generally raw when assimilated. Please clarify.*

  After "For noise reduction at high altitudes, raw bending angle profiles are initialized with background data" we added:

  leading to optimized bending angle profiles (note that raw bending angles are assimilated in numerical weather prediction systems).

- *Page 4: "The RO retrieval ... " Temperature, and several other profiles can also be derived from RO without using auxiliary information. Please clarify this statement, mention 1DVar.*

  To clarify this statement we rewrote the paragraph and mentioned the 1DVar. The concerning paragraph reads now:

Neglecting the moist contribution of refractivity in a so-called "dry air retrieval" yields atmospheric dry density profiles. Dry pressure profiles as a function of altitude, geopotential height profiles as a function of dry pressure altitude, and dry temperature profiles as a function of altitude are then calculated using the hydrostatic equation and the equation of state.
The assumption of dry air is valid where water vapor density is low, i.e., above ≈14 km at low latitudes and ≈9 km at high latitudes (Foelsche et al. 2008; Scherllin-Pirscher et al. 2011). In this case dry air parameters are essentially physical parameters. Below, however, the proportion of water vapor becomes significant and the difference between physical and dry temperature can reach several tens of kelvins in the lower troposphere (Foelsche et al. 2008; Scherllin-Pirscher et al. 2011). In this case auxiliary information is required for the retrieval of physical atmospheric parameters, e.g, through a one-dimensional variational (1DVar) method. Temperature, pressure, and water vapor are then derived using auxiliary temperature and/or humidity data as provided, e.g., by operational weather analysis centers (Healy and Eyre 2000).

- *Page 6: "The UCAR data processing ..." I would argue that a LEO orbit is not a level 0, and in the next sentence this is stated correctly.*

  We more precisely state now:

  The UCAR data processing as described by Kuo et al. (2004) and Ho et al. (2009) starts with raw GPS amplitude and phase measurements as well as raw GPS and LEO orbit tracking data (level 0 data).

- *Page 6: "Level 1 processing ..." Should be the other way round, first orbit, then excess phase processing.*

  We rewrote the sentence. It now reads:

  Level 1 processing comprises the reconstruction of precise LEO and GPS position and velocity vectors as well as the determination of atmospheric excess phase profiles.

- *Page 7: "In this study ..." What data from CHAMP, GRACE is used in your study, all of 2007 to 2009? Is there a reason why this COSMIC data is of higher quality?*

  In the first version of this paper we did not include CHAMP and GRACE data retrieved at UCAR, we only used F3C data. However, we now included CHAMP data (which are available until September 2008) and GRACE data.

  We rewrote the sentence. It now reads:

  In this study we use high quality CHAMP, GRACE-A, and F3C data from 2008 and 2009 (CHAMP data are only available until September 2008) with data versions 2009.2650 (CHAMP) and 2010.2640 (GRACE-A and F3C) from UCAR.

  Data quality is affected by the antenna quality (while GRACE-A and CHAMP carry helix-type antennas, F3C uses more advanced multi-element path antennas), the clock quality (while GRACE-A has an ultra-stable oscillator, which allows to perform zero differencing, CHAMP and F3C clocks are less stable, which requires single differencing to remove clock errors), and tracking mode (CHAMP and GRACE-A receivers operate in closed-loop mode, optionally with fly-wheeling in the lower to mid troposphere, F3C receivers operate in open-loop mode in the lower troposphere).

Bending angle noise at high altitudes is an indicator of receiver quality. Pirscher (2010) and Foelsche et al. (2011) compared bending angle noise of different satellites between 65 km and 80 km and found that CHAMP bending angle noise is about 1.5 to 2 times larger than GRACE and COSMIC bending angle noise.

We address this matter now and added the following statements in the revised manuscript text, in the abstract:

Above 35 km the increase of the CHAMP raw bending angle observational error is more pronounced than that of GRACE-A and F3C leading to a larger observational error of about 1 % at 42 km.

page 11, section 3.1:

Above about 42 km CHAMP raw bending angle observational error exceeds that of the other satellites by 1 %. This mainly derives from the larger bending angle noise observed in CHAMP data (Pirscher 2010; Foelsche et al. 2011).

page 15, section 3.3:

In the upper troposphere and lower stratosphere CHAMP and GRACE-A observational errors are slightly larger than F3C observational errors but differences rarely exceed 0.1 %.

and page 22, section 4:

Above about 35 km the CHAMP raw bending angle observational error increases stronger than that of GRACE-A and F3C. The difference exceeds 1 % above 42 km. Due to bending angle initialization at high altitudes, differences between the satellites above 35 km are smaller for other atmospheric parameters.

- *Figure 3: Are you actually using exactly the same occultations from both processing centres, at least at higher altitudes, for COSMIC comparisons?*

We do not use the same occultations from both processing centers but all available occultations in each month, which have passed quality control at the respective processing center. Since bending angles and refractivities of both data centers are in very good agreement, we feel confident that differences observed in further-derived atmospheric parameters are not caused by sampling issues (due to different quality criteria) and that it is not necessary to restrict the analysis to the same occultation events.

References

U. Foelsche, M. Borsche, A. K. Steiner, A. Gobiet, B. Pirscher, G. Kirchengast, J. Wickert, and T. Schmidt. Observing upper troposphere-lower stratosphere climate with radio occultation data from the CHAMP satellite. *Climate Dynamics*, 31:49–65, 2008. doi: 10.1007/s00382-007-0337-7.

U. Foelsche, B. Scherllin-Pirscher, F. Ladstädter, A. K. Steiner, and G. Kirchengast. Refractivity and temperature climate records from multiple radio occultation satellites consistent within 0.05 %. *Atmos. Measur. Tech. Discuss.*, 4:1593–1615, 2011. doi: 10.5194/amtd-4-1593-2011.

G. Gaspari and S. E. Cohn. Construction of correlation functions in two and three dimensions. *Quarterly Journal of the Royal Meteorological Society*, 125:723–757, 1999. doi: 10.1002/qj.49712555417.

S. B. Healy and J. R. Eyre. Retrieving temperature, water vapour and surface pressure information from refractive-index profiles derived by radio occultation: A simulation study. *Quarterly Journal of the Royal Meteorological Society*, 126(566):1661–1683, 2000.

S.-P. Ho, G. Kirchengast, S. Leroy, J. Wickert, A. J. Mannucci, A. K. Steiner, D. Hunt, W. Schreiner, S. Sokolovskiy, C. Ao, M. Borsche, A. von Engeln, U. Foelsche, S. Heise, B. Iijima, Y.-H. Kuo, E. R. Kursinski, B. Pirscher, M. Ringer, C. Rocken, and T. Schmidt. Estimating the uncertainty of using GPS radio occultation data for climate monitoring: Intercomparison of CHAMP refractivity climate records from 2002 to 2006 from different data centers. *Journal of Geophysical Research*, 114:D23107, 2009. doi: 10.1029/2009JD011969.

Y.-H. Kuo, T.-K. Wee, S. Sokolovskiy, C. Rocken, W. Schreiner, D. Hunt, and R. A. Anthes. Inversion and error estimation of GPS radio occultation data. *Journal of the Meteorological Society of Japan*, 82:1B, 2004.

B. Pirscher. *Multi-satellite climatologies of fundamental atmospheric variables from radio occultation and their validation (Ph.D. thesis)*. Wegener Center Verlag Graz, 2010. ISBN 978-3-9502940-3-3. Sci. Rep. 33-2010.

B. Scherllin-Pirscher, G. Kirchengast, A. K. Steiner, Y.-H. Kuo, and U. Foelsche. Quantifying uncertainty in climatological fields from GPS radio occultation: An empirical-analytical error model. *Atmos. Measur. Tech. Discuss.*, 4:2749–2788, 2011. doi: 10.5194/amtd-4-2749-2011.

A. K. Steiner and G. Kirchengast. Error analysis of GNSS radio occultation data based on ensembles of profiles from end-to-end simulations. *Journal of Geophysical Research*, 110:D15307, 2005. doi: 10.1029/2004JD005251.

A. K. Steiner, A. Löscher, and G. Kirchengast. Error characteristics of refractivity profiles retrieved from CHAMP radio occultation data. In U. Foelsche, G. Kirchengast, and A. K. Steiner, editors, *Atmosphere and Climate: Studies by Occultation Methods*, pages 27–36. Springer-Verlag, 2006.